The NO 2 vibronic levels near the X 2 A 1 –A 2 B 2 conical intersection: Jet cooled laser induced fluorescence between 11680 and 13900 cm−1

Antoine Delon and Remy Jost

Citation: The Journal of Chemical Physics **110**, 4300 (1999); doi: 10.1063/1.478313
View online: http://dx.doi.org/10.1063/1.478313
View Table of Contents: http://scitation.aip.org/content/aip/journal/jcp/110/9?ver=pdfcov
Published by the AIP Publishing

The NO_2 vibronic levels near the $X^2A_1-A^2B_2$ conical intersection: Jet cooled laser induced fluorescence between 11 680 and 13 900 cm^{-1}

Antoine Delon and Remy Jost[a)]
Grenoble High Magnetic Field Laboratory, BP 166, F-38042 Grenoble Cedex 09, France

(Received 26 May 1998; accepted 25 November 1998)

Following our previous LIF [J. Chem. Phys. **95**, 5701, (1991) and **103**, 1732 (1995)] and ICLAS [Chem. Phys. **190**, 207 (1995)] studies on NO_2, we observed by LIF the NO_2 vibronic levels between 11 680 and 13 900 cm^{-1}. These observations allow us to characterize the vibronic levels resulting from the conical intersection between the $X\,^2A_1$ and $A\,^2B_2$ electronic PESs. Globally, we observed by LIF 78 vibronic levels of B_2 vibronic symmetry, among which 61 had previously been observed by ICLAS. Conversely, one vibronic level observed at 13 088 cm^{-1} by ICLAS has not been observed by LIF. The 17 new levels have been observed thanks to a better sensitivity (about a factor 10) and resolution (0.3 GHz). The LIF intensities range over four orders of magnitude. The 79 (78+1) observed vibronic levels represent 83% of the 95 levels of B_2 vibronic symmetry calculated in that range; 85 $X\,^2A_1$ levels of b_2 vibrational symmetry and 10 $A\,^2B_2$ levels of a_1 vibrational symmetry. The missing levels are expected to have a weak $A\,^2B_2$ electronic character and then a very weak intensity. Consequently, these missing levels are expected not to be significantly shifted by $X\,^2A_1-A\,^2B_2$ vibronic interaction. In addition, 85 hot bands have been observed by LIF in the same range (among which only 15 have been observed by ICLAS). For most of the vibronic levels, the rotational constants (*A,B*) and spin splittings have been determined from their few lowest rotational levels. The zero order vibronic levels can be classified according to a polyad number, $N=N(\text{bend})+2N(\text{stretch})$. The present results cover the polyads four to seven. This experimental data, combined with laser induced dispersed fluorescence spectra (LIDFS), [J. Chem. Phys. **108**, 6638 (1998)] which give access to polyads one to five, contributes to a quantitative interpretation of the strong interaction between the $X\,^2A_1$ and $A\,^2B_2$ PESs. The integrated density of states of vibronic levels of B_2 symmetry is carefully discussed up to 19 360 cm^{-1} and the next neighbor spacing distribution (NNDS) is presented for a (almost?) complete set of 65 levels located between 12 500 and 13 860 cm^{-1}. These data contributes to the characterization of the transition from regularity, below 10 000 cm^{-1}, to quantum chaos, which is fully developed above ~16 500 cm^{-1} within the NO_2 vibronic degrees of freedom. © *1999 American Institute of Physics.* [S0021-9606(99)01509-3]

I. INTRODUCTION

NO_2 is well known for its conical intersection between the $X\,^2A_1$ and $A\,^2B_2$ potential energy surfaces (PESs).[1–3] However, a quantitative analysis and interpretation of its vibronic spectrum is still a challenge. There are conceptual difficulties in calculating the vibronic energy levels in the presence of a conical intersection[4–8] and there are no molecules for which a well-documented experimental set of vibronic levels exists close to a conical intersection. We have already studied the NO_2 spectrum by LIDFS,[9,10] ICLAS,[11] and LIF.[12,13] This molecule seems to be the best known example where the effects of a conical intersection can be both experimentally observed[11–22] and calculated.[23–26] There is now a large amount of experimental data at high energy where chaotic properties have been observed.[11–13,20–22] The energy range in which a quantitative and detailed analysis seems to be possible is located around and above 10 000 cm^{-1}, where the zero order $A\,^2B_2$ vibrational levels are very sparse, and the ones of the $X\,^2A_1$ state can be reasonably extrapolated from those lying at lower energy and which have been observed by LIDFS.[9,10] Unfortunately, the 10 000–14 000 cm^{-1} energy range is difficult to observe, mainly because the direct excitation corresponds to very weak Franck–Condon factors.[25–27] The LIDFS method allows us to access to this energy range, but only for levels of A_1 rovibronic symmetry (both A_1 and B_2 vibronic symmetries are observed[9,10]), while the LIF, for which only B_2 vibronic symmetry is observed,[11–22] gives access only to A_2 rovibronic symmetry.[28] This paper reports our experimental effort to observe the near IR range which corresponds to very weak absorption. This weakness has been overcome by the use of a powerful Ti:Sa laser, a slit jet (instead of a pinhole) and the detection of the fluorescence in the near IR with a LN_2 cooled germanium detector. At room temperature, the red and near IR part of the NO_2 absorption spectrum is very dense and irregular. Consequently, only six vibronic bands have been analyzed; Brand *et al.*,[29(a),29(b)] at 11 960 cm^{-1} and 15 435 cm^{-1}, Merer and Hallin[30–32] at 11 960, 12 100, and 13 511 cm^{-1} and Perrin *et al.*[33,34] at 13 184, 13 396, and

a)Author to whom correspondence should be addressed. Electronic mail: jost@polycnrs-gre.fr

13 511 cm^{-1}. These bands are the dominant ones in our LIF spectrum. Locally, the near IR range of the NO_2 absorption spectrum has also been studied with a bolometer detection.[35] The very high resolution of this technique allows for the resolving of the hyperfine structures which are typically lower than 100 MHz. The concatenation of vibronic energies measured by LIDFS,[9,10] and/or by ICLAS,[11] and/or by LIF (this paper) gives an almost complete ensemble of 214 vibronic energy levels of B_2 symmetry from the ground state up to 13 860 cm^{-1} (224 B_2 levels are calculated in that range). This allows a meaningful level spacing statistical analysis.

II. EXPERIMENT

The LIF experimental setup is analogous to the one used previously.[12,13] A schematic view of the experiment is shown in Fig. 1 of Ref. 9. However, three major changes should be noted; (i) a monomode Ti–Sa laser (Coherent 899) is used instead of a dye laser, (ii) a slit jet is used instead of a pinhole jet, and (iii), a LN_2 cooled germanium detector is used instead of a PMT because the fluorescence is shifted in the near IR. The NO_2 molecules (from 2% to 5%) seeded in argon (0.4 bar) are rotationally cooled in a cw supersonic slit jet expansion (2 cm×20 microns). The vibronic bands in the near IR are similar to the ones previously observed in the visible range (see Figs. 1 and 2 of Ref. 12 or figures in Refs. 14–20). The weakness of the absorption NO_2 spectrum in the near IR (Refs. 36–41) is overcome owing to the high column density of molecules in the slit jet; the collected fluorescence is typically 90 times stronger in a slit jet compared with our 100 μm standard pinhole jet. This increase is due to three effects; (i) the angular distribution of the jet density around the jet axis is about 10 times narrower compared to the one of a pinhole jet; consequently the Doppler width is about ten times narrower and the overlap with the spectral distribution of the single mode laser is ten times higher than for a pinhole jet and, (ii) the maximum flux (integrated along the slit) of NO_2 molecules (without important formation of $Ar–NO_2$ complexes!) is larger than for a pinhole jet. This is partly due to the fact that the jet density decreases only as $1/d$ (the distance from the nozzle), and not as $1/d^2$ for a pinhole jet. The drawback of the slit jet is the poorer rotational cooling. However, the rotational cooling is not critical in the near IR part of the NO_2 spectrum because the vibronic density is significantly lower than in the visible range. The observed rotational temperature is roughly 15–20 K. Note that the rotational populations deviate from thermal equilibrium, especially when different K manifolds are analyzed. The broader partition function reduces the intensity of the stronger lines by a factor of 2–3. The estimated vibrational temperature is about 200 K, much higher than the rotational temperature. The 2 W cw power of our monomode Ti:Sa laser is typically five times stronger than the power used in the visible range. Altogether, the fluorescence is expected to be 250 times stronger than in our previous visible LIF study with a pinhole. On the other hand, the detection of the fluorescence is less efficient in the near IR than in the visible because the fluorescence is shifted to the red. In addition, the lifetime of the vibronic levels excited in the near IR are significantly longer than those excited in the visible range. The main limitation of the signal to noise ratio when using a germanium detector is due to the cosmic rays. We have used either a cw or a low frequency lock-in detection with roughly the same S/N ratio. Our experimental spectrum is composed of about two thousand adjacent scans of 1 cm^{-1} where the wavelength of the lines are approximately measured during the scan. Then, each line expected to belong to the $K=0$ manifold of vibronic band is measured with our 8 digits homemade lambdameter. This allows to make secure rotational assignments by combination differences using the known rotational energy levels of the ground state.[42] The uncertainty on combination differences is typically 0.003 cm^{-1}. The absolute uncertainty is estimated to be 0.02 cm^{-1}. Our relative intensities of vibronic band are determined only from the sum of the (usually two) R_0 lines. These intensities are difficult to interpret because they depend on the fluorescence spectral range and the lifetime of each vibronic level which are rather long (up to 100 μs) for the vibronic levels studied here. This uncomfortable situation explains why the ratio of LIF and ICLAS (absorption) intensities fluctuate up to one order of magnitude. Fortunately, the observed intensities range over four orders of magnitude and the local hierarchy of intensities is roughly the same when they are classified according to their LIF or ICLAS intensities.

III. RESULTS

The core of this paper is the list of 79 vibronic levels of $^2B_2$ symmetry, observed from 11 680 to 13 900 cm^{-1} and given in Table I and shown in Fig. 1. The 85 hot bands, which have been observed in the same spectral range, are listed in Table II for completeness, but they are not discussed here because we are mainly interested in the vibronic energies. The ratios between hot and cold intensities will be compared with Franck–Condon calculations in the future. The discrimination between cold and hot bands was possible owing to our previous ICLAS observations in the 11 200–16 100 cm^{-1} energy range. The criteria used to assign the hot bands was not only the energy shift between the cold and the hot band origins, but also the rotational and spin splittings, which are specific to each vibronic level.[10–21] With these criteria, the cold or hot character of the observed vibronic bands is very secure. Generally, these new LIF results agree with the previous ICLAS results. However, there is a global improvement for the 61 vibronic levels observed previously by ICLAS because the LIF resolution is typically ten times better than the one of ICLAS and numerous spin splittings are now resolved. The line positions are also more accurate by a factor of 10. This allows for discrimination between accidental coincidences between lines belonging respectively to hot and cold bands. In addition, many $K=1$ manifold not observed by ICLAS have been measured and analyzed. The corresponding ''A'' constant are listed in Table I. The comparison of the band origins and of the ''A'' constants for the vibronic levels which have been analyzed previously at room temperature[29–34] shows huge discrepancies. This can be explained by the very irregular rotational structure of some vibronic bands of NO_2 in this energy range, mainly for vibronic bands having a strong $A\,^2B_2$ character. At room temperature, the low rotational quantum numbers are not ob-

TABLE I. List of vibronic energies (origins of cold band only), A rotational constants (deduced from the splitting between $K=0$ and $K=1$ stacks) and LIF and/or ICLAS intensities for 79 levels of $^2B_2$ vibronic symmetry observed by LIF from 11 680 to 13 860 cm^{-1}. The vibronic level observed only by ICLAS is marked with a $. The 14 levels observed with a bolometer detection (Ref. 35) are marked with §. The missing entries for the A and/or $\overline{B}$ rotational constants and for the $\overline{\epsilon}$ spin constant correspond to irregular rotational structures and/or irregular spin splittings. The few levels observed previously by absorption at room temperature are discussed in the text.

Vibronic energy (cm^{-1})	Intensities LIF (a.u.)	Intensities ICLAS (a.u.)	Rotational constants A (cm^{-1})	Rotational constants $\overline{B}$ (cm^{-1})	Spin constants $\overline{\epsilon}$ (cm^{-1})
11 694.41	0.24	0.15	8.0[b]	0.446	0.078
11 807.80§	1.00	0.3	13.7[b]	0.420	0.003
11 833.38[a]	0.02	0.07			
11 847.75§	1.00	0.2	13.4[b]	0.400	0.052
11 960.70§	20.00	1.2	8.09	0.460	−0.200
12 059.01	0.25	0.1	10.8[b]	0.420	−0.093
12 084.26	0.18	0.007	9.0[b]	0.408	0.022
12 100.90§	2.54	0.4	11.41	0.426	0.008
12 177.06	0.31	0.15	9.2[b]	0.446	0.023
12 263.28	0.60	0.15	11.8[b]	0.417	−0.009
12 293.79	0.02		10.0[b]	0.407	−0.025
12 320.66	0.02		7.8[b]	0.442	
12 340.52§	0.40	0.25	15.44	0.434	0.024
12 410.71	0.70	0.2	9.7[b]	0.417	−0.032
12 446.03§	1.00	0.3	8.53	0.435	0.026
12 516.24	0.10	0.006	8.4[b]	0.410	0.009
12 559.70	0.10	0.01	17.2[a,b]	0.392	0.063
12 567.80	0.80		19.1[a,b]	0.393	[c]
12 575.57	2.00	0.1	11.3[a,b]	0.460	−0.023
12 578.61	0.70		8.3[a,b]		[d]
12 594.51	0.60				[c]
12 600.44	2.00	0.1	10.9[b]	0.440	0.420
12 637.09	2.50	0.05	7.9[b]	0.417	0.000
12 658.38§	12.20	1.0	8.65[b]	0.439	0.029
12 668.94§	5.10	0.15	8.15[b]	0.406	0.000
12 702.62	7.70	0.15	8.05	0.406	0.033
12 723.87§	11.20	0.3	8.46	0.419	−0.064
12 739.83	3.90	0.2	8.71	0.420	0.025
12 770.32	0.80	0.1		0.457	[c]
12 775.46	0.70	0.02	11.0[b]		[d]
12 812.31	1.40		6.7[b]	0.43	[d]
12 856.10[a]	0.20				[c]
12 863.18	0.60	0.06	10.0[b]	0.426	0.005
12 871.08	0.10				[c]
12 887.86	0.10	0.005	8.5[b]	0.450	[c]
12 906.85	0.50	0.01	7.7[b]	0.405	0.000
12 916.29	0.60	0.03	9.60	0.410	0.017
12 923.29	0.10			0.419	−0.018
12 985.84	0.90	0.03	11.4[b]	0.4[a]	[c]
13 008.84	7.70	0.3	9.96	0.427	−0.067
13 020.74	1.70	0.04	16.0[b]	0.410	0.000
13 047.51	0.80	0.04		0.400	0.020
13 088.36$		0.05		0.418	0.031
13 132.30	0.20				[c]
13 138.87	0.20		9.1[b]	0.413	−0.025
13 158.32	3.30	0.05	8.29	0.410	0.011
13 184.57§	18.50	0.2	12.75	0.423	0.018
13 208.59	4.40	0.1	8.22	0.400	0.000
13 222.89	5.80	0.12	8.2[b]	0.420	0.022
13 264.33	5.60	0.1	7.6[b]	0.400	0.005
13 285.22	25.00	0.25	12.58	0.424	0.090
13 303.17	1.50	0.05	9.5		[c]
13 340.14	1.90	0.01		0.426	0.004
13 352.68§	7.80	0.25	10.6[a]	0.402	0.009
13 395.71§	250.00	2.5	9.85	0.445	0.041
13 398.10	18.00				−0.060
13 406.18	32.00		8.24	0.452	−0.030
13 427.82	16.00	0.1			[d]
13 443.25	0.30				0.029

TABLE I. (*Continued.*)

Vibronic energy (cm^{-1})	Intensities LIF (a.u.)	Intensities ICLAS (a.u.)	Rotational constants A (cm^{-1})	Rotational constants $\overline{B}$ (cm^{-1})	Spin constant $\overline{\epsilon}$ (cm^{-1})
13 477.04§	13.90	0.8	7.94	0.418	−0.009
13 510.92§	122.00	0.8	16.0	0.430	0.090
13 552.80	18.30	0.4	9.73	0.406	−0.022
13 576.76	2.70	0.04			[c]
13 591.40	40.00	0.4	9.28	0.403	0.086
13 621.90	2.30	0.04			[d]
13 641.58	1.00	0.04		0.417	0.022
13 650.22[a]	0.60				[c]
13 672.96	0.80			0.419	0.015
13 680.30§	11.00	0.3	8.50	0.420	0.030
13 691.43	2.00				[d]
13 713.59	1.10	0.05		0.404	[c]
13 730.70	0.50				[c]
13 742.14	12.80	0.25		0.390	[d]
13 766.68	14.30	0.3	9.66		[d]
13 783.50	7.20	0.15	7.08	0.403	0.004
13 791.25	2.40	0.04			[c]
13 810.84	53.00	1.2	9.31	0.418	[d]
13 831.16	23.30	0.5	9.20	0.416	0.060
13 858.38	12.10	0.2		0.425	0.050

[a]Doubtful.
[b]Using LIDFS results.
[c]Irregular spin splittings.
[d]More than two spin components on the $K=0$, $N=1$, and/or $N=3$ levels.

served, while large quantum numbers are not observed in the jet. Our ''*A*'' constants are determined from the splitting between $K=0$ and $K=1$, while the room temperature ''*A*'' constants are values averaged over a manifold of several K values which suffer rovibronic perturbations. Our band origins correspond to extrapolation from $N=1, K=0$ to $N=0, K=0$ (which does not exist[28]) while the band origins determined from room temperature measurements necessitate larger extrapolations. As a result, apparent shifts up to few cm^{-1} exist for the band origins and for the ''*A*'' constants between room temperature and present jet observations. At higher energy (in the visible range), the situation is worse and rotational assignments are possible only locally. Note that only J ($J=N+S$) remains a good quantum number. Note that hyperfine splittings ($I=1$) are not resolved and the nuclear spin may be ignored. The reason of the irregular structure lies mainly in the strong vibronic couplings *and* in the difference between the large ''*A*'' constants of the high levels of the $X\,^2A_1$ ground state (from 8 to 20 cm^{-1} according to the number of quanta in the bending mode[10]) and the low ''*A*'' constants of the zero order low lying levels of the $A\,^2B_2$ state (expected to be of the order of 3 cm^{-1} from *ab initio* calculations[1,2]).

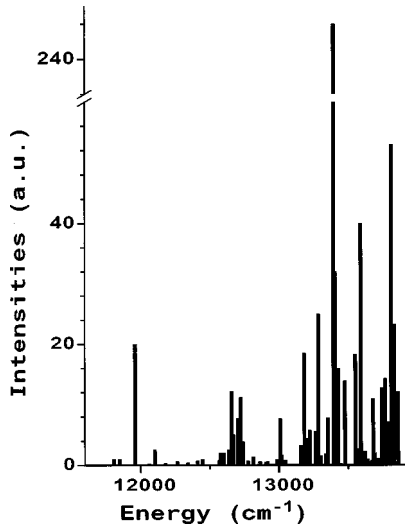

FIG. 1. Stick spectrum of $^2B_2$ vibronic bands (cold band only) between 11 680 and 13 860 cm^{-1}. Note the LIF intensity axis breaking which is used because of the large intensity of the vibronic band at 13 395 cm^{-1}; These intensities are only indicative as discussed in the text. Note the huge fluctuations of the intensity ratio between ICLAS (absorption) and LIF intensities given in Table I.

It is not possible to quantitatively compare the LIF and ICLAS intensities in the absence of lifetime measurements. However, an interesting feature emerges from the comparison between LIF and ICLAS intensities, especially for the levels located between 11 680 and 12 300 cm^{-1} [i.e. around the (0,3,0) bright level located near 11 960 cm^{-1}]; the normalized LIF intensities are proportional to the square of the ICLAS (absorption intensities). This can be explained by the following assumption: the LIF intensities are proportional not only to the absorption, but also to the inverse of the lifetime because the long-lived molecules can escape the observation region before fluorescing. The inverse of lifetime, that is the rate of spontaneous emission, is expected to be proportional to the square of the coefficient of the $A\,^2B_2$ electronic wave function in each eigenstate. Since the absorption [i.e., ICLAS intensities and the first step (laser excitation) of the LIF intensities] is also proportional to this

TABLE II. List of 85 hot bands observed by LIF from 11 680 to 13 860 cm^{-1} with their LIF intensities and their initial $X\,^2A_1$ vibrational level 0,1 for (0,1,0), 0,2 for (0,2,0) and 1,0 for (1,0,0).

Band origin (cm^{-1})	Initial level v_1,v_2	Intensity (a.u.)
11 686.23	0,2	0.18
11 696.40	0,1	0.71
11 908.71	0,1	1.83
11 952.98	0,1	1.64
11 974.22	0,1	2.05
11 990.20	0,1	0.63
12 012.60	0,2	0.50
12 054.50	0,2	0.12
12 075.90	1,0	0.63
12 093.00	0,2	0.30
12 191.12	1,0	0.10
12 236.19	0,1	0.10
12 243.80	0,2	0.03
12 271.09	0,1	0.10
12 292.91	0,2	0.03
12 297.86	0,1	0.10
12 312.50	0,2	0.30
12 332.82	0,2	0.10
12 338.71	0,1	0.10
12 360.04	0,2	0.10
12 408.67	0,1	0.40
12 434.92	0,1	0.90
12 458.94	0,1	0.40
12 473.24	0,1	0.40
12 486.19	0,2	0.10
12 495.62	0,2	0.20
12 504.93	0,2	0.20
12 514.68	0,1	0.30
12 524.02	0,2	0.30
12 535.57	0,1	2.10
12 553.52	0,1	0.20
12 602.89	0,1	1.60
12 622.54	0,2	0.20
12 609.39	0,2	0.90
12 639.59	0,2	0.30
12 646.06	0,1	13.30
12 676.90	0,1	0.70
12 679.00	0,2	0.20
12 755.74	0,2	0.30
12 761.27	0,1	7.20
12 803.14	0,1	1.20
12 808.93	1,0	1.10
12 818.40	0,2	0.40
12 827.34	0,1	0.10
12 841.73	0,1	3.40
12 847.61	0,2	0.80
12 852.70	1,0	0.30
12 857.65	1,0	0.60
12 872.06	0,1	0.20
12 891.90	0,1	0.10
12 930.63	0,1	0.80
12 941.30	0,2	0.10
12 963.93	0,1	0.10
12 992.49	0,1	0.70
13 017.24	0,1	1.10
13 033.85	0,1	0.70
13 041.60	0,1	0.50
13 051.64	0,2	0.40
13 061.19	0,1	5.20
13 078.05	0,2	1.10
13 081.44	0,1	2.40
13 108.71	0,1	0.80
13 119.86	1,0	0.30
13 234.89	0,1	2.90
13 244.31	0,1	6.70
13 253.52	0,1	3.80
13 272.71	0,1	11.70
13 320.91	0,1	2.60
13 337.12	0,2	0.90
13 379.04	0,1	28.00
13 388.28	0,1	1.60
13 460.26	1,0	0.20
13 465.40	0,1	1.80
13 493.72	1,0	0.60
13 504.43	0,1	2.00
13 536.34	0,1	1.00
13 561.22	0,1	1.10
13 596.32	0,1	17.00
13 614.55	1,0	2.90
13 665.07	0,2	0.90
13 689.90	0,1	7.10
13 715.51	0,2	0.80
13 800.33	0,1	6.90
13 826.66	0,1	33.00
13 886.11	0,2	1.10

weight, this makes the LIF signal proportional to the square of the ICLAS signal. This is in agreement with the fact that the $X\,^2A_1$–$A\,^2B_2$ coupling is sparse at low energy (in the near IR range) and that most of the vibronic eigenstates have a dominant $X\,^2A_1$ character with a weak $A\,^2B_2$ contamination. This effect has been discussed by Douglas.[43] At higher energies, the LIF intensities tend to be proportional to the ICLAS intensities because the lifetimes are shorter and the LIF signal observed on a length of about 5 mm along the jet axis (this corresponds to a duration of 7 μs after the laser excitation) is not significantly reduced by the long lifetime effect mentioned above.

IV. THE DENSITY OF STATES AND CORRELATION PROPERTIES

In order to analyze the properties of the levels of B_2 vibronic symmetry, we need to know which part of the complete set they represent. The numbers of levels discussed below are summarized in Table III, on which the energy range up to 19 360 cm^{-1} is analyzed. The $^2B_2$ vibronic levels result from the interaction of two sets; the set of high vibrational levels of b_2 symmetry of the $X\,^2A_1$ ground state, and the set of a_1 symmetry of the $A\,^2B_2$ state. It is reasonable to assume that the vibronic interactions shift and mix these zero order states, but do not significantly change the level density. The zero order vibrational energies of the $X\,^2A_1$ state can be calculated by extrapolation from the energies of the levels lying at lower energy. The complete set of the $X\,^2A_1$ vibrational levels have been observed by LIDFS (Ref. 10) and assigned up to 11 700 cm^{-1} for the a_1 vibronic symmetry (171 levels) and up to 11 000 cm^{-1} for the B_2 vibronic sym-

TABLE III. Numbers of B_2 vibronic levels observed and calculated in various energy ranges.

Energy range (cm^{-1})	Number of B_2 levels Observed by LIDFS	ICLAS	LIF	ICLAS+LIF	Total[a]	Calculated	Missing	
0–11 000	104	⋯	⋯	⋯	104	104	0	(0%)
11 000–11 680	15	4	⋯	4	16	19	3	(16%)
11 680–12 500	19	13	15	15	24	30	6	(20%)
12 500–13 860	14	48	63	64	64	65	1	(1.5%)
11 680–13 860	33	61	78	79	88	95	7	(7%)
13 860–14 640	⋯	26	[b]	26	26	45	19	(42%)
14 640–16 125	⋯	83	49[c]	88	88	116	28	(25%)
0–16 125	152	174[d]	126	200	323	380	57	(15%)
16 125–16 580	⋯	⋯	27	27	27	40	13	(32%)
16 580–19 360	⋯	⋯	315	315	315	328	13	(4%)
0–19 360	152	174	470	541	665	748	83	(11%)

[a]The levels which have been observed by two or three techniques are counted only once.
[b]The levels observed by LIF in Ref. 20 are not taken into account (see Table III of Ref. 11).
[c]The levels observed by LIF in Ref. 14 are taken into account.
[d]The band at 13 614.57 cm^{-1} and erroneously listed in Table I of Ref. 11 is a hot band from the (1,0,0) level and has been removed.

metry (104 levels). In this energy range, few of these levels seems to be shifted by the vibronic interactions and the fit of the unshifted levels with a 24 parameter Dunham model gives a typical rms of 1 cm^{-1}. Then, the levels calculated with these Dunham parameters are a good estimate of the zero order energy (without vibronic interactions) of these levels. As a result, there are 85 predicted levels of b_2 symmetry (B_2 vibronic symmetry) between 11 680 and 13 860 cm^{-1} for the $X\,^2A_1$ state. Similarly, the number of vibrational levels of the $A\,^2B_2$ state can be estimated from the position of the (0,0,0) levels observed at 9734 cm^{-1} [and for which the deperturbed energy is estimated at 9722 cm^{-1} (Ref. 10)] and from estimated harmonic vibrational frequencies, $\omega_1 = 1420\,cm^{-1}$, $\omega_2 = 740\,cm^{-1}$, and $\omega_3 = 1500\,cm^{-1}$. These values are rather imprecise, but the number of B_2 levels of a_1 vibrational symmetry in the 11 680–13 860 cm^{-1} energy range is only 10 and this number is stable when the three vibrational frequencies are varied by a few percent. The sum of the two electronic contributions is then 95 (85 + 10) levels of B_2 vibronic symmetry, to be compared with 79 levels observed by LIF and/or by ICLAS (i.e., 83%, see Table III). In addition, numerous vibronic levels of B_2 symmetry have also been observed by LIDFS,[10] from the (0,0,1) of the $X\,^2A_1$ state up to 13 900 cm^{-1}. In fact, our LIDF spectra allow us to observe the $K=1$ manifold from which the extrapolation to $K=0$ is rather vague when the ''A'' constant is not known. However, the mean B_2 vibronic spacing is of the order of 25 cm^{-1} around 12 000 cm^{-1} and most of the ''A'' constants are between 7 and 16 cm^{-1}. Then, the correspondence between the $K=1$ manifold (observed by LIDFS) and the $K=0$ (observed by LIF and/or by ICLAS) is unambiguous in most of the case. For example, between 11 680 and 12 500 cm^{-1}, there are 19 B_2 vibronic levels ($K=1$ only) observed by LIDFS, 9 of which cannot be associated with one of the vibronic levels observed by LIF or ICLAS and listed in Table I. This number of levels can be compared with 15 missing levels (30 calculated and 15 observed) according to the calculations presented above. We have concatenated the B_2 vibronic band origins (vibronic energies) observed by LIDFS with the ones observed by LIF and/or by ICLAS (listed in Table I only from 11 680 to 13 860 cm^{-1}) up to 19 360 cm^{-1}. The corresponding numbers of levels are given in Table III and are presented in Fig. 2 only up to 16 125 cm^{-1} in order to visualize the two regions in which there are numerous missing levels. Note that many vibronic levels have been observed by two (and sometime three) techniques. As a result, 323 B_2 vibronic levels have been observed up to 16 125 cm^{-1} to be compared with 38 calculated levels. Below typically 20 000 cm^{-1}, the numbers of levels calculated with our Dunham expansion are in very good agreement with the ones calculated from *ab*

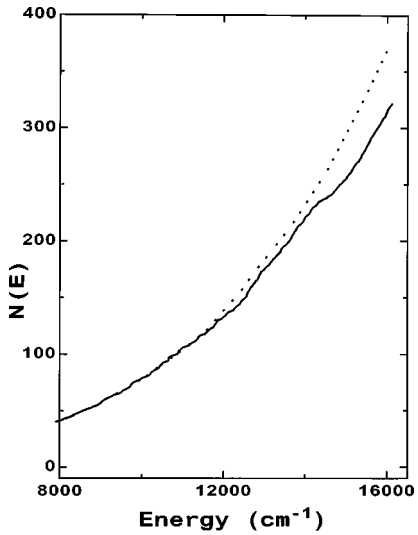

FIG. 2. Comparison between the observed (full line) and calculated (dotted line) integrated density ($N(E)$) of vibronic levels of B_2 symmetry from 8 000 to 16 125 cm^{-1}. Below 8 000 cm^{-1} the two curves are almost identical. The corresponding numbers are given in Table III. Note that there is no missing levels from 0 to 11 000 cm^{-1}, few missing levels between 11 000 and 12 500 cm^{-1}, almost no missing levels between 12 500 and 13 860 cm^{-1} [because the observed $N(E)$ is parallel to the calculated $N(E)$], many missing levels between 13 860 and 14 640 cm^{-1}, and few missing levels from 14 640 and 16 125 cm^{-1}. Figure 4 of Ref. 13 shows $N(E)$ above 16 125 cm^{-1}.

initio PES.[24,25] An examination of the integrated density of states, $N(E)$, of B_2 vibronic levels (see Fig. 2) shows that (i) there is no missing level below 11 000 cm^{-1}; (ii) there are about 9 missing level between 11 000 and 12 500 cm^{-1}; (iii) there are almost no missing levels from 12 500 to 13 860 cm^{-1} (64 observed levels and 65 calculated levels); (iv) there is a large fraction of missing levels around 14 300 cm^{-1}: about 25 missing levels between 13 860 and 14 640 cm^{-1}; (v) there are about 30 missing levels (about 25%) from 14 640 to 16 125 cm^{-1}.

We have performed the statistical analysis of energy spacings only for the 12 500–13 860 cm^{-1} energy range, in which the set of 64 levels is almost complete. We have unfolded[44] the $N(E)$ with the formula 6 of Ref. 13 which is shown in Fig. 2 (dotted line). A cubic power of energy [taken from the zero point energy of the PES, and not from the (0,0,0) level] is a very good local approximation of formula (6) of Ref. 13. The next neighbor spacing distribution (NNSD) (Ref. 44) has a standard deviation of 0.63 (or $\langle S^2 \rangle = 1.4$) and $\langle S^3 \rangle = 2.49$. These values are slightly larger than the values expected for a Wigner distribution, but it is not possible to draw a more precise conclusion with this limited set of 64 levels. However, we may notice that the NNDS of the upper half of this set (between 13 200 and 13 860 cm^{-1}) is closer to a Wigner distribution than the lower half indicating (the statistic is poor!) a smooth transition towards a Wigner distribution with increasing energy. This set is too limited for analyzing the long range correlations. The intensities increase significantly from 12 500 cm^{-1} to 13 860 cm^{-1} with two broad maxima around 12 700 and 13 400 cm^{-1} where the zero order, ''bright,'' $A\,^2B_2$ vibrational levels are located.[10] It is then necessary to ''unfold'' the intensities before constructing the intensity distribution.[44] After various reasonable unfoldings, the intensity distributions (not shown) are in rough agreement with the Porter–Thomas distribution. In contrast, we observed a significant broader intensity distribution for the vibronic levels located below 12 500 cm^{-1}. This is consistent with the fact that the zero order $A\,^2B_2$ levels are weakly coupled to the set of dark $X\,^2A_1$ levels below 12 500 cm^{-1}. Below this energy, the large number of missing levels in the LIF and ICLAS spectra is partly due to the weakness of the optical transitions (the absorption cross section decreases with decreasing energy), but also to the fact that some vibronic levels have an almost pure $X\,^2A_1$ electronic character (they are almost pure dark levels) or, conversely, they have a very weak $A\,^2B_2$ electronic character. This interpretation, which is in agreement with our LIDFS results[10] on A_1 and B_2 vibronic levels located between 9 000 and 12 500 cm^{-1}, is discussed in the next section. It should be noted that the set of 83 B_2 vibronic levels observed by ICLAS and located between 14 640 and 16 125 cm^{-1} has been previously analyzed in Ref. 11. Another set of 315 B_2 vibronic levels has been observed by LIF from 16 580 to 19 360 cm^{-1}.[13] The correlation properties of these two sets are close to the ones of a Gaussian orthogonal ensemble (GOE).[13,44] Up to 19 360 cm^{-1} there are 665 observed and 748 calculated B_2 vibronic levels; this means that there are 83 missing levels. Most of these missing levels are located between 14 000 and 14 640 cm^{-1} and between 16 125 and 16 580 cm^{-1}, mostly because the NO_2 absorption cross section is weak in these ranges.[36–41]

V. THE $X\,^2A_1$–$A\,^2B_2$ VIBRONIC INTERACTION

The LIF results presented above and the previous LIDFS (Ref. 10) and ICLAS (Ref. 11) results can be used to characterize and to understand the $X\,^2A_1$–$A\,^2B_2$ vibronic interaction. In this section, we want to draw some conclusions on the global properties of this vibronic interactions due to the conical intersection of the potential energy surfaces of the $X\,^2A_1$ and $A\,^2B_2$ states which explains the complexity of the visible NO_2 spectrum, from 10 000 cm^{-1} up to the limit of dissociation and above. We will mainly discuss the low energy range (9 700–12 500 cm^{-1}), where the vibronic interactions are localized and easier to analyze from the theoretical point of view. In the high energy range, above ~12 500 cm^{-1}, mainly statistical methods can be used.[11–13,21,24] The zero order vibrational levels of the $A\,^2B_2$ state are organized into polyads because $\omega_1 \cong 2\omega_2 \cong \omega_3$. This polyad structure is shown in Fig. 2 of Ref. 10. The analysis presented in Ref. 10 shows that the vibronic interaction can be treated within isolated polyads, at least up to the fourth polyad. It should be noted that these four lowest polyads of B_2 symmetry have no excitation of the antisymmetric stretching mode. The first polyad, in which the antisymmetric stretch of the $A\,^2B_2$ state is excited [namely, the (0,0,2) level], is the fifth polyad around 12 650 cm^{-1}. This polyad includes the (0,4,0), the (1,2,0) and the (2,0,0,) in addition to the (0,0,2) level. It seems that the NNSD (and possibly other statistical properties) changes rather abruptly from the fourth polyad (around 11 960 cm^{-1}) to the fifth polyad (around 12 650 cm^{-1}). This observation is valid for the intensity distribution of our cold excitation spectrum and is confirmed by the room temperature absorption spectrum which changes abruptly when going from the fourth to the fifth polyad.[36,38,39]

The $X\,^2A_1$–$A\,^2B_2$ conical intersection has been studied by *ab initio* calculations,[1–3] and the related vibronic interaction by Cederbaum,[23(a)] via stationary state calculations, with a crude two electronic states-3D harmonic oscillator model, in which the coupling is oversimplified by a lambda Q_3 operator. Recently, Leonardi *et al.*[23(b)] used a corrected *ab initio* PES to calculate the vibronic energy levels. Their results are in quantitative agreement with the experimental observations up to 9300 cm^{-1} and in semiquantitative agreement up to at least 12 500 cm^{-1}. This model is useful to make a quantitative analysis of our experimental data. However, the examination of the eigenvalues and mixing coefficients of the Siena group[23(d)] indicates that their vibronic mixings are globally stronger than those deduced from our crude analysis of experimental results presented in the previous section. One of the main difficulties is due to the fact that *all* the vibrational levels of the $A\,^2B_2$ state interact with the high vibrational levels of the $X\,^2A_1$ state. It is then not possible to determine precisely the ''true'' frequency of the three modes of the $A\,^2B_2$ state and then to predict the zero order energy of the higher vibrational energy levels of that state. In other words, the zero order energies of the $A\,^2B_2$ state *and* the parameter(s) of the $X\,^2A_1$–$A\,^2B_2$ interaction should be de-

termined simultaneously from the experimental data. Taking into account the large number of free parameters (zero order energies, and off diagonal matrix elements), it is not yet possible to built a *quantitative* model from our experimental data. Clearly, both new experimental results (including vibronic energies, rotational constants, and absorption intensities) and a realistic model Hamiltonian with some adjustable parameters are necessary to make a *quantitative* analysis of the vibronic interaction in NO_2. This quantitative analysis seems to be possible up to 12 300 cm^{-1} (the upper limit of the fourth polyad) in terms of individual levels (quantitative interpretation of each eigenvalue and eigenfunction). In contrast, above this energy, only a statistical analysis in term of mixing coefficients, dilution factors seems to be possible. We note that the''A'' rotational constants (in fact we determine only the energy splittings between the $K=0$ and $K=1$ manifolds) are very useful, in addition to the energies, for the characterization of the eigenstates. Polyads of A_1 vibronic symmetry (b_2 vibrational symmetry of the $A\,^2B_2$ state) can also be considered. These polyads seems to be almost degenerate with those of B_2 symmetry because $\omega_3 \cong \omega_1$. The first polyad contains only the (0,0,1) level (may be observed at 11 115.5 cm^{-1}; see Sec. IV B of Ref. 10), the second polyad contains only the (0,1,1) level expected around 11 850 cm^{-1}, the third polyad contains the (1,0,1) and the (0,2,1) levels expected around 12 600 cm^{-1}, and so on. Unfortunately, we have too little information on these polyads of A_1 vibronic symmetry. An IR- near-IR double resonance experiment using the (0,0,1) level of the ground state as intermediate state would allow us to observe selectively these levels of A_1 vibronic symmetry with a significant $A\,^2B_2$ character. Note that LIF and ICLAS allow us to observe only vibronic levels of B_2 symmetry having a $A\,^2B_2$ character while LIDFS allows us to observe both A_1 and B_2 symmetries in an energy which is limited experimentally by the CCD camera.[10]

VI. CONCLUSIONS AND PERSPECTIVES

This LIF paper mainly gives spectroscopic information (energies, LIF intensities, rotational constants, spin splittings) on the dense set of vibrational levels of $^2B_2$ vibronic symmetry located between 11 680 and 13 900 cm^{-1}. This set complements those obtained previously at lower energy by LIDFS (Ref. 10) (the complete sets of vibronic levels of A_1 and B_2 symmetries have been obtained up to 11 000 cm^{-1}), and at higher energy, by ICLAS (Ref. 11) and LIF.[12–22] The observed intensities and level spacing statistics indicate a qualitative evolution of the vibronic interactions around 12 500 cm^{-1}, when going from the fourth to the fifth polyad of the $A\,^2B_2$ state. By using the cavity ring down spectroscopy (CRDS) technique, with which preliminary results have been obtained, it seems possible to observe the vibronic level of $^2B_2$ vibronic symmetry which are still missing above 11 000 cm^{-1} and then to get the complete set of $^2B_2$ vibronic levels of NO_2 up to 19 600 cm^{-1}. A quantitative analysis of the vibronic energies (B_2 vibronic symmetry only) up to the fourth polyad of the $A\,^2B_2$ state (i.e., up to 12 300 cm^{-1}) now seems possible. This will allow us to go beyond statistical analysis, which is a frustrating ''black box'' that does not give either spectroscopic nor precise dynamic information. This data can be used to test the *ab initio* methods devoted to the calculation of vibronic levels in presence of a conical intersection.[3–8,23,24]

ACKNOWLEDGMENTS

We thank M. Abbouti Temsamani, M. Barthelemy, J. Nygard, for their contribution to the collection of the LIF spectra and data analysis. We also thank Professor C. Petrongolo and D. F. Santoro of the University of Siena, Professor Ch. Schlier and R. F. Salzgeber of the University of Freiburg, and Professor M. Jacon of the University of Reims for communicating their calculated vibronic energy levels prior to publication and for discussions. The Grenoble High Magnetic Field Laboratory (G.H.M.F.L.) is ''Laboratoire conventionné aux universités UJF et INP de Grenoble.''

[1] C. F. Jackels and E. R. Davidson, J. Chem. Phys. **64**, 2908 (1976).
[2] G. D. Gillispie, A. V. Khan, A. C. Wahl, R. P. Hosteny, and M. Krauss, J. Chem. Phys. **63**, 3425 (1975).
[3] E. Leonardi, C. Petrongolo, V. Keshari, G. Hirsch, and R. Buenker, Mol. Phys. **82**, 553 (1994), and previous papers of this series.
[4] H. C. Longuet-Higgins, Adv. Spectrosc. **2**, 429 (1961).
[5] C. A. Mead, Chem. Phys. **49**, 23 (1980).
[6] H. Koppel, W. Domcke, and L. S. Cederbaum, Adv. Chem. Phys. **57**, 59 (1984).
[7] B. Kendrick and R. T Pack, J. Chem. Phys. **104**, 7475 (1996); **104**, 7502 (1996); **106**, 3519 (1997).
[8] B. Kendrick, Phys. Rev. Lett. **79**, 2431 (1997).
[9] A. Delon and R. Jost, J. Chem. Phys. **95**, 5686 (1991).
[10] B. Kirmse, A. Delon, and R. Jost, J. Chem. Phys. **108**, 6638 (1998).
[11] R. Georges, A. Delon, F. Bylicki, R. Jost, A. Campargue, A. Charvat, M. Chenevier, and F. Stoeckel, Chem. Phys. **190**, 207 (1995).
[12] A. Delon, M. Lombardi, and R. Jost, J. Chem. Phys. **95**, 5701 (1991).
[13] R. Georges, A. Delon, and R. Jost, J. Chem. Phys. **103**, 1732 (1995).
[14] R. Smalley, L. Wharton, and D. H. Levy, J. Chem. Phys. **63**, 4977 (1975).
[15] F. Paech, R. Schmiedl, and W. Demtröder, J. Chem. Phys. **63**, 4369 (1975).
[16] H. J. Foth, H. J. Vedder, and W. Demtröder, J. Mol. Spectrosc. **88**, 109 (1981).
[17] H. J. Vedder, M. Schwarz, H. J. Foth, and W. Demtröder, J. Mol. Spectrosc. **97**, 92 (1983).
[18] G. Persch, H. J. Vedder, and W. Demtröder, J. Mol. Spectrosc. **123**, 356 (1987).
[19] G. Persch, H. J. Vedder, and W. Demtröder, J. Mol. Spectrosc. **123**, 356 (1987).
[20] G. Persch, E. Mehdizadeh, W. Demtröder, Th. Zimmermann, H. Köppel, and L. S. Cederbaum, Ber. Bunsenges. Phys. Chem. **92**, 312 (1988).
[21] Th. Zimmermann, H. Köppel, L. S. Cederbaum, G. Persch, and W. Demtröder, Phys. Rev. Lett. **61**, 3 (1988).
[22] J. Miyawaki, K. Yamanouchi, and S. Tsuchiya, J. Chem. Phys. **101**, 4505 (1994).
[23] (a) E. Haller, H. Köppel, and L. S. Cederbaum, J. Mol. Spectrosc. **111**, 377 (1985); (b) E. Leonardi, C. Petrongolo, G. Hirsch, and R. Buenker, J. Chem. Phys. **105**, 9051 (1996); (c) F. Santoro, *ibid.* **109**, 1824 (1998); (d) R. Brandi, F. Santoro, and C. Petrongolo, Chem. Phys. **225**, 55 (1997); (private communication).
[24] R. F. Salzgeber, V. Mandelshtam, Ch. Schlier, and H. S. Taylor, J. Chem. Phys. **109**, 937 (1998).
[25] G. D. Gillispie and A. V. Khan, J. Chem. Phys. **65**, 1624 (1976).
[26] G. Xie and G. Yan, Mol. Phys. **88**, 1349 (1996).
[27] J. Lievin, A. Delon, and R. Jost, J. Chem. Phys. **108**, 8931 (1998).
[28] P. Bunker, *Molecular Symmetry and Spectroscopy* (Academic, London, 1979).
[29] (a) J. C. D. Brand, W. H. Chan, and J. L. Hardwick, J. Mol. Spectrosc. **56**, 309 (1975); (b) J. C. D. Brand, K. J. Cross, and A. R. Hoy, Can. J. Phys. **57**, 428 (1979).
[30] A. J. Merer and K. E. Hallin, Can. J. Phys. **56**, 838 (1978).
[31] A. J. Merer and K. E. Hallin, Can. J. Phys. **56**, 1502 (1978).

[32] K. E. Hallin and A. J. Merer, Can. J. Phys. **55**, 2102 (1977).
[33] A. Perrin, C. Camy-Peyret, J. M. Flaud, and P. Luc, J. Mol. Spectrosc. **88**, 237 (1981).
[34] A. Perrin, C. Camy-Peyret, J. M. Flaud, and P. Luc, Can. J. Phys. **60**, 1288 (1982).
[35] C. A. Biesheuvel, D. H. A. ter Steege, J. Bultuis, M. H. M. Janssen, J. G. Snijders, and S. Stolte, Chem. Phys. Lett. **269**, 515 (1997); C. A. Biesheuvel, ''High-resolution laser spectroscopy of the nitrogen molecule,'' thesis, Free University of Amsterdam, The Netherlands, January 1998.
[36] J. Orphal, S. Voigt, S. Dreher, J. P. Burrows, R. Jost, and A. Delon, J. Chem. Phys. (to be published).
[37] W. Schneider, G. K. Moortgat, G. S. Tyndall, and J. P. Burrows, J. Photochem. Photobiol., A **40**, 195 (1987).
[38] J. P. Burrows, A. Richter, A. Dehn, B. Deters, S. Himmelmann, S. Voigt, and J. Orphal, J. Quant. Spectrosc. Radiat. Transf. (to be published).
[39] A. C. Vandaele, C. Hermans, P. C. Simon, M. Carleer, R. Colin, S. Fally, M. F. Merienne, A. Jenouvier, and B. Coquard, J. Quant. Spectrosc. Radiat. Transf. **59**, 174 (1998).
[40] J. W. Harder, J. W. Brault, P. V. Johnston, and G. H. Mount, J. Geophys. Res. **102**, 3861 (1997).
[41] B. Kirmse, A. Delon, and R. Jost, J. Geophys. Res. **102**, 16089 (1997).
[42] J. M. Brown, T. C. Steimle, M. E. Coles, and R. F. Curl, J. Chem. Phys. **74**, 3668 (1981).
[43] A. E. Douglas, J. Chem. Phys. **45**, 1007 (1966).
[44] T. A. Brody, J. Flores, J. B. French, P. A. Mello, A. Pandey, and S. S. M. Wong, Rev. Mod. Phys. **53**, 385 (1981).